Robotica (2006) volume 24, pp. 105–112. © 2005 Cambridge University Press
doi:10.1017/S0263574705001906 Printed in the United Kingdom

Positional kinematics of humanoid arms

Jadran Lenarčič* and Nives Klopčar

Jožef Stefan Institute, Dept. of Automatics, Biocybernetics and Robotics, Jamova 39, 1000 Ljubljana (Slovenia)

(Received in Final Form: April 4, 2005)

SUMMARY

We present the positional abilities of a humanoid manipulator based on an improved kinematical model of the human arm. This was synthesized from electro-optical measurements of healthy female and male subjects. The model possesses three joints: inner shoulder joint, outer shoulder joint and elbow joint. The first functions as the human sternoclavicular joint, the second functions as the human glenohumeral joint, and the last replicates the human humeroulnar rotation. There are three links included, the forearm and the upper arm link which are of a constant length, and the shoulder link which is expandable. Mathematical interrelations between the joint coordinates are also taken into consideration. We determined the reachability of a humanoid arm, treated its orienting redundancy in the shoulder complex and the positional redundancy in the shoulder-elbow complexes, and discussed optimum configurations in executing different tasks. The results are important for the design and control of humanoid robots, in medicine and sports.

KEYWORDS: Humanoid arm; Humanoid manipulator; Reachability; Reachable workspace; Kinematical model; Human arm; Self-motion.

I. INTRODUCTION

In the last decade, the study of humanoid arms and humanoid manipulation has become important, in particular in service robotics and in rehabilitation engineering. Humanoid robots are conceptualized with the objective to help humans in diverse everyday activities, where human-like morphology is an important advantage. In rehabilitation and other areas of medicine and sports, the knowledge on humanoid arms and manipulation can serve to develop new evaluation methods, rehabilitation protocols, or new types of biomedical devices.

Current designs of humanoids include simplified arms that are able to replicate only basic functions of the human arm. There is, therefore, a need to study mathematical and physical models, as well as appropriate performance and design criteria, that could enable a more profound analysis of the human arm performances and development of more capable and efficient humanoid arms. Significant progress has been made in the design and control of humanoid robots,[1] especially in dynamic walking of full-body humanoids.[2] Some attention has also been given to the humanoid manipulation. Investigations in this area are usually focused on real time animation of the human arm,[3,4] where kinematic and dynamic models are used to efficiently mathematically represent or estimate the human arm pose and its self-motion ability.[5,6] For this purpose, the number of degrees of freedom in the arm mechanism is reduced. Typically, the human shoulder complex is approximated by a spherical joint which may in other applications, for example in medicine or in design of humanoid robots, represent a drawback.[7,8] Very few authors studied the shoulder girdle for humanoid robots.[9–12]

In this article, we investigate the principal positional characteristics of a humanoid arm. The ability of the arm to position the center of the wrist in space is studied, while the function of the wrist and the hand are not considered. For this purpose we take advantage of a kinematical model of the human arm which we developed in reference [13] and which enables us to accurately compute and visualize the reach of the wrist. The inputs to the model are the arm proportions and the ranges of motion in the joints of the shoulder and of the elbow complexes which have to be measured for each specific subject in a prescribed reference pose of the arm. The main advantage of the introduced kinematical model is in the usage of two displaced spherical joints in the shoulder complex and in the usage of joint limits as functions of joint coordinates. Usually, only one spherical or universal joint is used to replicate the shoulder in the designs of humanoids and constant joint limits are imposed. The introduced improvements enable us to compute and replicate human manipulation characteristics more accurately.

In the paper, we compute the envelope of the reachable workspace. We propose how to resolve the mechanism's redundancy and how to avoid or how to take advantage of mechanism's singularities. The ability of the self-motion of the arm is discussed in order to emphasize its capacity to adapt to different tasks. The presented results are primarily meant for design and control purposes of humanoid robots but can also find their application in medicine and sports, in particular in physiotherapy, where this new knowledge can serve to better understand the human arm motion.

II. HUMANOID ARM KINEMATICS

The human arm is composed of a skeletal system with several bones, tendons and muscles which form different combinations of serial and parallel kinematic chains. Single joint motions are mechanically interrelated through the operation of many actuators that drive the same joint and actuators that drive more joints simultaneously.

* Corresponding author. E-mail: jadran.lenarcic@ijs.si

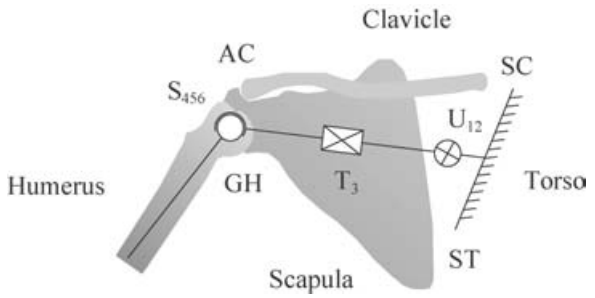

Fig. 1. Shoulder complex approximation (right arm – frontal view).

The kinematical model of the human arm with the associated dependencies of joint limits which we use in this investigation was proposed in reference [13]. In this model, the innermost portion of the shoulder is the shoulder girdle.[14,15] It consists of two bones, the clavicle and the scapula, which connect the humerus to the torso (Fig. 1). The motion of the girdle is enabled by the scapulothoracic, sternoclavicular, and acromioclavicular joint denoted by ST, SC, AC, respectively.

Since the bones of the shoulder girdle move conjointly, it can be seen as a parallel mechanism (as it will be showed later) in which the scapula has the role of the platform and the torso the role of the base. One leg of this parallel mechanism is the articulation between the scapula and the torso, the other leg is the clavicle. It was demonstrated that the girdle produces two independent degrees of freedom which characterize the motion of the scapula and are mostly rotatory. The principal motion of the girdle can thus be modelled by using an universal joint U_{12} combined with a dependent translation T_3 which models the change in length between the torso and the glenohumeral joint. Only the two rotations of the first joint need to be controlled while the translation is dependent on the inclination of the upper arm.[12]

The glenohumeral joint attaches the upper arm to the shoulder and is a ball-and-socket joint. The glenohumeral joint has a wide range of motion because the socket is small and the joint capsule provides little additional support. We can approximate it by three rotations concentrated in a spherical joint S_{456} with the center of rotations placed in the center of the head of the humerus. The shoulder complex thus contributes to the humerus five degrees of freedom. Mechanically, the shoulder complex can be seen as a double pointing-orienting system (a system of a dislocated universal and a spherical joint) enabling a complete orientation of the upper arm.[11]

The elbow complex and the forearm is a system of articulations between three bones, which are the ulna, the radius and the humerus (Fig. 2). The elbow joint is a compound joint consisting of the humeroulnar joint HU and the humeroradial joint HR. The humeroulnar joint allows the ulna to rotate with respect to the humerus. The humeroradial joint HR is a ball-and-socket joint between the capitulum of the humerus and the radial head. The ulna and radius are connected at both ends. The superior (proximal) radioulnar joint RU_S is between the radial head and the radial notch of ulna. The inferior (distal) radioulnar joint RU_I is between the distal ends of the radius and ulna. The radioulnar joints can

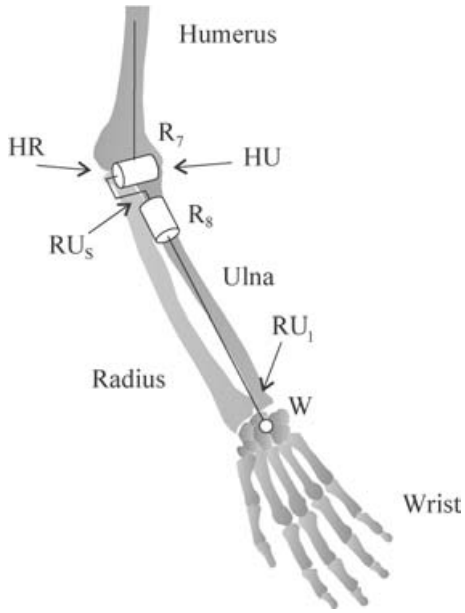

Fig. 2. Elbow complex approximation (right arm – frontal view).

be seen as pivot joints allowing the radius to rotate about a longitudinal axis the ulna.

The forearm is a complex parallel mechanism[16] whose mechanical function can be replaced by two simple rotations R_7 and R_8 as shown in Fig. 2. Here, rotation R_7 replicates the elbow flexion extension, and rotation R_8 replicates the pronation supination movement of the forearm. In Fig. 2, point W is understood as the center of the wrist and lies between process styloideus ulnae and process styloideus radii.

II.1. Kinematical model

The basic mathematical objective is to determine the position of reference point W. In the presented kinematical model (Fig. 3), the inner shoulder joint U_{12} and the outer shoulder joint S_{456} are replaced by a series of rotations intersecting in one point which are R_1, R_2 and R_4, R_5, R_6, respectively. They are connected by a dependent translation T_3. In the elbow complex, only rotation R_7, representing the elbow flexion-extension movement, is included because the motion of supination-pronation R_8 does not influence the position of point W. Note that the outer shoulder joint is positioned in the center of the glenohumeral joint, while the inner shoulder joint lies on the intersection of an posterior-anterior axis, which passes through the center of the sternoclavicular joint, and a medial-lateral axis, which passes through the center of the glenohumeral joint.

Let us denote the joint coordinates by $q_1, \ldots, q_7$, where q_3 is a linear displacement, all others are joint angles. Parameter d_S represents the size of the shoulder and is the length between the inner shoulder joint and the outer shoulder joint (when $q_3 = 0$), d_H is the size of the humerus and is the length between the outer shoulder joint and the elbow joint, d_F is the size of the forearm and is the length between the elbow joint and reference point W. The reference coordinate frame is attached to the torso in the center of the inner shoulder joint. In the reference pose of the arm (all joint coordinates

https://doi.org/10.1017/S0263574705001906 Published online by Cambridge University Press

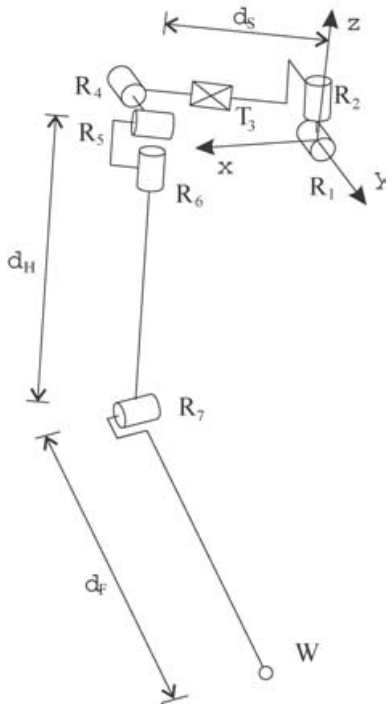

Fig. 3. Kinematical model referred to spatial position of point W.

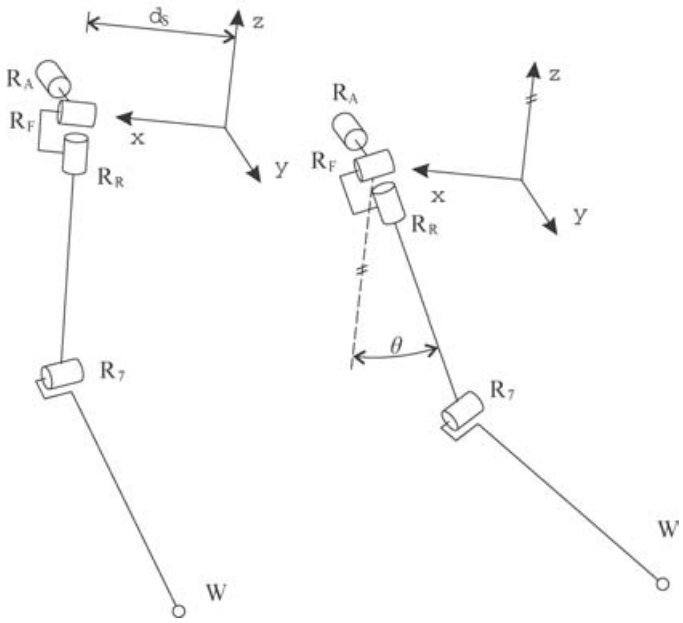

Fig. 4. Simplified kinematical model referred to spatial position of point W.

are zero) R_2 is parallel to y, R_2 is parallel to z, T_3 is parallel to x, R_4 is parallel to y, R_5 is parallel to x, R_6 is parallel to z, and R_7 is parallel to x, while the shoulder link (d_S) is parallel to x, the upper arm link (d_H) is parallel to z, and the forearm link (d_F) is parallel to axis y.

The spatial position of point W with respect to the reference coordinate frame can be obtained by the following well know equation

$$\mathbf{p}_W = \mathbf{A}_1\mathbf{A}_2(\mathbf{d}_S + \mathbf{A}_4\mathbf{A}_5\mathbf{A}_6(\mathbf{d}_H + \mathbf{A}_7\mathbf{d}_F)), \tag{1}$$

where vectors

$$\begin{aligned} \mathbf{d}_S &= (d_S + q_3, 0, 0)^T, \\ \mathbf{d}_H &= (0, 0, -d_H)^T, \\ \mathbf{d}_F &= (0, d_F, 0)^T, \end{aligned} \tag{2}$$

are associated with the link lengths and $\mathbf{A}_i$ are the 3×3 rotation matrices. They are functions of joint angles and can be computed by

$$\mathbf{A}_i = \mathbf{I} + \mathbf{\Delta}_i \sin q_i + \mathbf{\Delta}_i^2(1 - \cos q_i), \tag{3}$$

where matrix $\mathbf{\Delta}_i$ contains the components of the unit joint vector $\mathbf{e}_i = (e_{ix}, e_{iy}, e_{iz})^T$ as follows

$$\mathbf{\Delta}_i = \begin{bmatrix} 0 & -e_{iz} & e_{iy} \\ e_{iz} & 0 & -e_{ix} \\ -e_{iy} & e_{ix} & 0 \end{bmatrix}, \tag{4}$$

In our case we have

$$\begin{aligned} \mathbf{e}_1 &= (0, 1, 0)^T, \\ \mathbf{e}_2 &= (0, 0, 1)^T, \\ \mathbf{e}_4 &= (0, 1, 0)^T, \\ \mathbf{e}_5 &= (1, 0, 0)^T, \\ \mathbf{e}_6 &= (0, 0, 1)^T, \\ \mathbf{e}_7 &= (1, 0, 0)^T. \end{aligned} \tag{5}$$

II.2. Joint limits

It is known that the limits of joint coordinates $q_1, \ldots, q_7$ cannot be expressed by fixed intervals for a humanoid arm. Usually, the limits of a joint coordinate depend on the current pose of the arm. The determination of these dependencies is an extremely complex problem and has never completely been solved. The most accurate approach so far was introduced in reference [13], where a simplified kinematical model which replicates standard anatomical motions usually examined in physiotherapy and sports was used as shown in Fig. 4. It possesses only three perpendicular revolute joints to describe the motion of the whole shoulder complex, including the glenohumeral joint and the shoulder girdle. In this simplified model, R_A is associated with the shoulder abduction-adduction movement, R_F with the shoulder flexion-extension movement, and R_R with the internal-external shoulder rotation. Clearly, R_A, R_F and R_R approximate the movements of the inner (R_1, R_2 and T_3) and the outer shoulder joint (R_4, R_5 and R_6). Let the coordinates of R_A, R_F, R_R be denoted by angles θ_A, θ_F, θ_R, respectively, and the related joint axes are

$$\begin{aligned} \mathbf{e}_A &= (0, 1, 0)^T, \\ \mathbf{e}_F &= (1, 0, 0)^T, \\ \mathbf{e}_R &= (0, 0, 1)^T. \end{aligned} \tag{6}$$

https://doi.org/10.1017/S0263574705001906 Published online by Cambridge University Press

The correspondent rotation matrices $\mathbf{A}_A$, $\mathbf{A}_F$, $\mathbf{A}_R$ can be obtained by Eq. 3.

It is assumed here that the lower and the upper limits of joint coordinates θ_A, θ_F, θ_R, and q_1, q_2, q_7 are known for a specific subject. The range of each coordinate is measured in the so-called reference pose of the arm, this is when all other joint coordinates are equal to zero. Note that such a measurement is relatively simple and is usually part of a standard measurement protocol in physiotherapy or sports. The obtained lower limits are θ_{Am}, θ_{Fm}, θ_{Rm}, q_{1m}, q_{2m}, q_{7m} and the upper limits are θ_{AM}, θ_{FM}, θ_{RM}, q_{1M}, q_{2M}, q_{7M}.

Accordingly to reference [17] the following is valid

$$\theta_A = (\theta_{Am}, \theta_{AM}), \tag{7}$$

$$\theta_F = \left(\theta_{Fm} + \frac{1}{3}\theta_A, \theta_{FM} - \frac{1}{6}\theta_A\right), \tag{8}$$

$$\theta_R = \left(\theta_{Rm} + \frac{7}{9}\theta_A - \frac{1}{9}\theta_F + \frac{4}{9\pi}\theta_A\theta_F, \theta_{RM} + \frac{4}{9}\theta_A - \frac{5}{9}\theta_F + \frac{10}{9\pi}\theta_A\theta_F\right). \tag{9}$$

In reference [13] we observed that the ranges of the inner shoulder joint rotations R_1, R_2 can be formulated as functions of the humeral elevation angle θ which is measured between the humeral axis and axis z as shown given in Fig. 4. Angle θ is given by

$$\theta = \arccos(\cos\theta_A \cos\theta_F). \tag{10}$$

The intervals of coordinates q_1 and q_2 as functions of θ are as follows

$$q_1 = \left(q_{1m} - \frac{3}{72}\theta + \frac{14}{36\pi}\theta^2, q_{1M} - \frac{1}{36}\theta + \frac{8}{36\pi}\theta^2\right), \tag{11}$$

$$q_2 = \left(q_{2m} + \frac{11}{72}\theta - \frac{8}{36\pi}\theta^2, q_{2M} + \frac{11}{72}\theta - \frac{14}{36\pi}\theta^2\right). \tag{12}$$

It is important to understand that the simplified kinematical model, which uses coordinates θ_A, θ_F, θ_R for the shoulder complex and disregards the contribution of the inner shoulder joint, primarily produces an error in the position of the mechanism but is quite accurate in terms of orientation. Thus, we can impose the following

$$\mathbf{A}_1\mathbf{A}_2\mathbf{A}_4\mathbf{A}_5\mathbf{A}_6 = \mathbf{A}_A\mathbf{A}_F\mathbf{A}_R, \tag{13}$$

in which it is required that both kinematical models produce the same orientation of the humerus. This relationship enables us to rewrite the position of point W given in Eq. 1 by

$$\mathbf{p}_W = \mathbf{A}_1\mathbf{A}_2\mathbf{d}_S + \mathbf{A}_A\mathbf{A}_F\mathbf{A}_R(\mathbf{d}_H + \mathbf{A}_7\mathbf{d}_F). \tag{14}$$

We have now two alternatives to compute the position of point W. One is by the use of Eq. 1 where the inputs are the values of coordinates $q_1, \ldots, q_7$. The other alternative is by the use of Eq. 14 where the inputs are θ_A, θ_F, θ_R and q_1, q_2, q_3, q_7. In both, however, we need to base our computation on the values of coordinates θ_A, θ_F, θ_R because their ranges of motion are known. If we want to use Eq. 1 we have first to compute coordinates q_4, q_5, q_6. This is done by reformulating Eq. 13 into

$$\mathbf{A}_4\mathbf{A}_5\mathbf{A}_6 = \mathbf{A}_2^T\mathbf{A}_1^T\mathbf{A}_A\mathbf{A}_F\mathbf{A}_R, \tag{15}$$

where it is understood that the matrices on the right hand side are known and that their product is a matrix of components a_{ij}. It then follows

$$\begin{aligned} q_4 &= \arctan_2 \frac{a_{13}}{a_{33}}, \\ q_5 &= -\arcsin a_{23}, \\ q_6 &= \arctan_2 \frac{a_{21}}{a_{22}}. \end{aligned} \tag{16}$$

An equivalent solution is

$$\begin{aligned} q_4' &= \arctan_2 \frac{a_{13}}{a_{33}} + \pi, \\ q_5' &= \arcsin a_{23} + \pi, \\ q_6' &= \arctan_2 \frac{a_{21}}{a_{22}} + \pi. \end{aligned} \tag{17}$$

In reference [13] we also developed the dependency of translation T_3 on angle θ

$$\frac{q_3}{d_S} = -\frac{6}{36\pi}\theta^2 + \frac{2}{36\pi}\theta, \tag{18}$$

while the range of the elbow joint is taken as fixed

$$q_7 = (q_{7m}, q_{7M}). \tag{19}$$

It is clear that the lower and the upper limits of the joint coordinates may vary among individuals as they are affected by age, sex, or eventual injuries.

III. POSITIONAL PROPERTIES OF A HUMANOID ARM

In anthropometric tables, for example in reference [18], one can find the lengths of the human arm segments relative to the hight of the subject h. Accordingly, the length of the shoulder girdle is $d_S = 0.129h$, of the upper arm is $d_H = 0.185h$, and of the forearm is $d_F = 0.146h$. By taking into account these sizes and the joint limits introduced in the previous section, it is easy to observe that point W cannot coly with the segments of the arm, including the shoulder segment. Moreover, the collisions between the segments of the arm, if we do not count the hand, are impossible.

III.1. Reachability and arm proportions

Once the kinematical model is known and the related joint ranges are determined, it is possible to obtain the whole volume of points in space which can be reached by the reference point W, the so-called reachable workspace. The computation of the reachable workspace can be formulated as an iterative procedure of a number of nested loops within which the values of joint angles are iterated throughout their ranges and the position of point W is computed for each combination of values of joint coordinates. In addition to these computations, the collisions between the segments of the arm and the body have to be taken into account. If an arm segment intersects with the body, the related position of W is eliminated.

https://doi.org/10.1017/S0263574705001906 Published online by Cambridge University Press

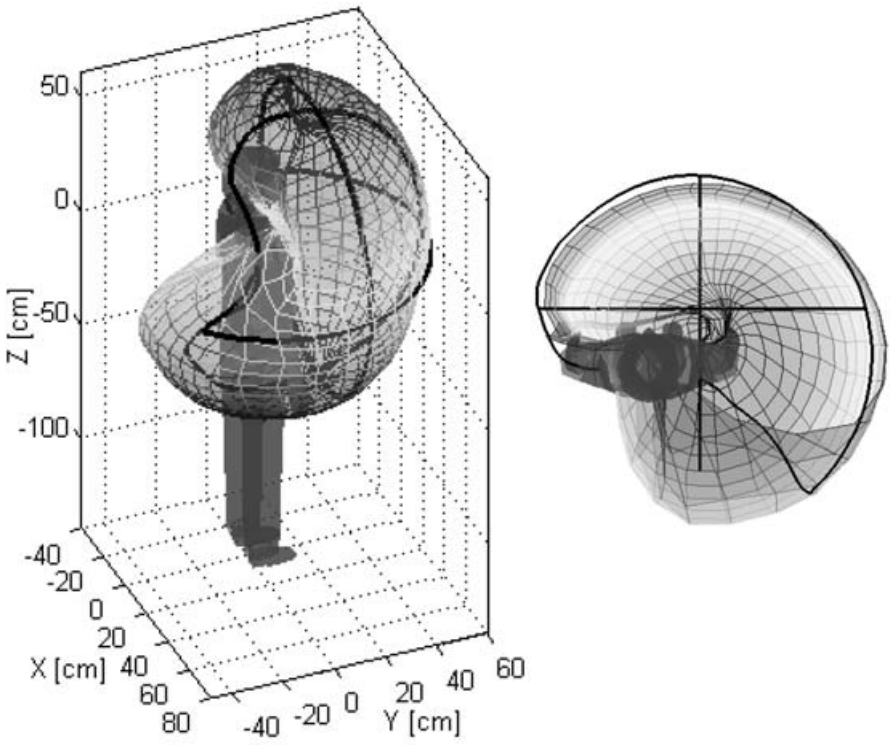

Fig. 5. Computed reachable workspace.

The outer loops are related to angles $\theta_A, \theta_F, \theta_R$ and for each triplet of their values we compute angle θ in order to obtain the ranges of coordinates q_1, q_2 and the value of coordinate q_3. When these are known, we proceed with additional iterations associated with coordinates q_1, q_2, and q_7. In each iteration, the position of point W is obtained by the use of Eq. 14. The result is a cloud of points in Cartesian space representing the insight of the reachable workspace. Usually, tens of thousands of iterations are needed to determine the whole set of points approximating the reachable workspace. The surface of the workspace is later interpolated and smoothed so that the workspace can effectually be visualized with different color textures, illuminated with different positions of light, or made transparent.

The following lower limits of joint coordinates were measured for a concrete human subject (in radians): $\theta_{Am} = -0.17$, $\theta_{Fm} = -1.05$, $\theta_{Rm} = -1.05$, $q_{1m} = -0.24$, $q_{2m} = -0.45$, $q_{7m} = -1.57$. The upper limits were (in radians): $\theta_{AM} = 2.97$, $\theta_{FM} = 2.97$, $\theta_{RM} = 1.57$, $q_{1M} = 0.52$, $q_{2M} = 0.52$, $q_{7M} = 1.05$. The corresponding enveloped of the reachable workspace of the right humanoid arm obtained based on the presented kinematical model is shown in Fig. 5 – hight $h = 175$ cm. The black lines superimposed onto the envelope were obtained by measuring the reach od the human arm of the same subject. The error is quite small and can additionally be minimized by more precise measurements.

The geometry of the reachable workspace depends on the arrangement of joints in the mechanism, ranges of joint coordinates and relative proportions between the link lengths. There were attempts in the past to synthesize an optimum mechanism which maximizes the workspace volume or produces a desired workspace form. Some authors affirmed that the maximum volume of the reachable workspace is obtained with the link lengths that are similar to the human arm proportions. In reference [19], the notion of workspace compactness was introduced in addition to the workspace volume – a more compact workspace is more round and with the same volume can provide more flexibility to solve different tasks. In a humanoid arm, as it was shown, the optimum ratio between the lengths of the forearm and the upper arm which maximizes the volume of the reachable workspace is similar to the one which maximizes the compactness. This isn't so in other types of mechanisms. This optimum ratio is similar to the human arm proportions. From this point of view, a humanoid manipulator appears to be more universal and flexible in executing spatial paths of different sizes and patterns.

Note that the determination of the reachable workspace in terms of a set of points in space includes a complete information on the positional ability of the arm, not only on the maximum reach but also of the insight properties. It can, therefore, serve for a deeper analysis, for example, one can plot the velocity (manipulability) ellipsoids throughout the workspace or study the sensitivity in different poses of the mechanism.

III.2. Girdle as a parallel mechanism

A parallel design of the mechanical shoulder girdle was first presented in,[12] where we described a mechanical system as shown in Fig. 6-left. The mechanism possesses a fixed base representing the torso and a movable platform representing the scapula holding the glenohumeral joint. The three outer legs connect the base and the platform through a passive spherical and universal joint and a driven translational joint. The central leg connects the platform and the base through a passive spherical joint and a driven translation. By driving the legs the mechanism can be expanded and oriented. The mechanism gives to the platform four degrees of freedom.

https://doi.org/10.1017/S0263574705001906 Published online by Cambridge University Press

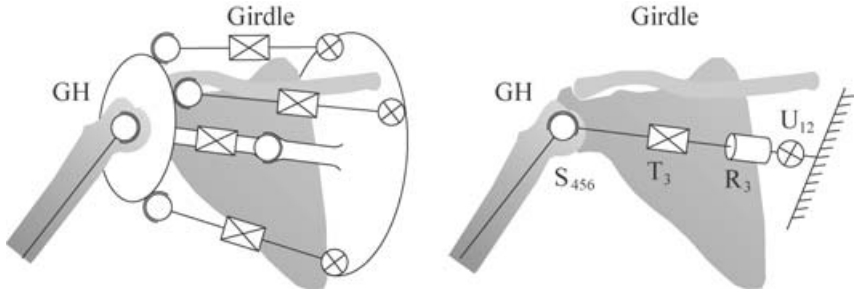

Fig. 6. The humanoid shoulder girdle with parallel kinematics.

This can be seen in Fig. 6-right, where a serial equivalent of this parallel mechanism is presented.

The relatively small ranges of motion that are requested in the girdle mechanism allow the usage of a parallel kinematic structure. The main advantage is that the parallel mechanism is more rigid and provides better accuracy and portability than a serial one. The generalized forces applied to the platform transform into longitudinal forces in the outer legs (it is not valid for the central leg). This is important since the mechanism must resist to the weight and dynamical forces of the whole arm and of the carried load. The translation of the central leg serves to regulate the distance between the glenohumeral joint which is dependent on the inclination of the platform as mentioned before. It can be observed that the difference between the mechanism in Fig. 6 and the mechanism in Fig. 1 is in an additional rotation R_3 about the shoulder axis.

In kinematic terms, the primary task of the human shoulder complex is to orient the upper arm. For this purpose the shoulder complex is kinematically redundant and for a given orientation of the upper arm the shoulder complex can produce an infinite repertoire of configurations. In humans, however, the shoulder girdle and the glenohumeral joint move conjointly. This motion is referred to as the shoulder rhythm and can be seen as coplanar.[11] In this motion, rotation R_3 has no anatomical role. Nevertheless, R_3 can be very useful for design and control purposes, since it can help to avoid the kinematic singularity in the spherical glenohumeral (outer shoulder) joint attached to the platform.

In the design of a humanoid mechanism, it is important to consider the fact that the outer shoulder joint is kinematically singular when R_5 rotates R_6 in a pose where it is parallel to R_4 (Fig. 7-left). This singularity reduces the number of operational degrees of freedom from three to two. In its neighborhood, the motion is ill-conditioned and extreme joint velocities are required to achieve a small change in the upper arm orientation. However, the singularity can be pushed out from the workspace defined by the ranges of joint coordinates as they were introduced in the previous section. It can be done by using rotation R_3 and by placing the outer shoulder joint so that the axis of rotation R_4 is inclined of about 60° with respect to the axis of R_3 or T_3, as shown in Fig. 7-right (original inclination is 90°).

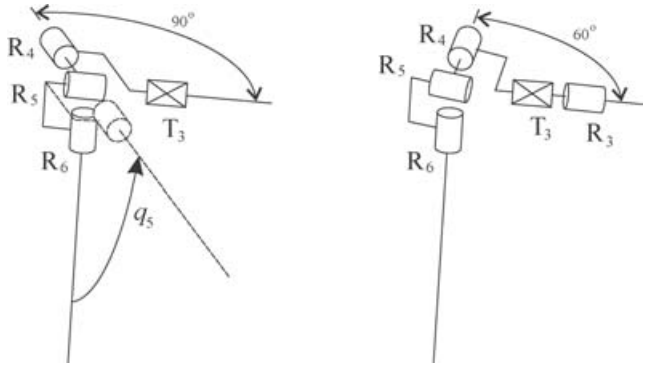

Fig. 7. Avoidance of singularity cone in outer shoulder joint.

III.3. Kinematic redundancy

Redundancy is a source of freedom because it enables to solve an assigned task in an infinite number of ways. From the viewpoint of positioning the wrist point W in space the human arm contains superfluous degrees of freedom and is, therefore, redundant. The described humanoid mechanism contains seven (or eight if R_3 is also included), but only three would be needed for positioning.

In order to better understand the humanoid motion, let us first consider the subtask of the primary task of positioning point W, which is the orienting of the upper arm. This subtask is designated to the shoulder complex. We model the shoulder complex as a system composed of two interrelated orienting systems, the inner shoulder joint, playing the role of the shoulder girdle, and the outer shoulder joint, playing the role of the glenohumeral joint. There is an offset between these two joints which is important for a proper operation of the shoulder. Its length is changing depending of the upper arm inclination.

For a full orientation of the upper arm only one spherical joint would be necessary. But the system of two displaced spherical joints introduces important advantages in the humanoid motion. The range of motion of the inner shoulder joint is about one third of those of the outer shoulder joint. Nevertheless, the workspace of the arm is reduced to less than 50% if the inner shoulder joint is locked. This is not only because the inner shoulder joint increases the orientation angles of the upper arm but also because the inner shoulder joint enables the arm to avoid collisions with the body. In terms of design, the distribution of the task of orientation into two joints is also very important because spherical joints are difficult to built and even more difficult to drive by parallel actuators. The usage of the displaced pair of joints also makes possible to prevent singularity configurations as described in the pervious section.

The humanoid shoulder motion is dominated by the interconnection of the inner and the outer shoulder joint. In producing a desired orientation of the upper arm they move in conjunction with each other. Their motion is

https://doi.org/10.1017/S0263574705001906 Published online by Cambridge University Press

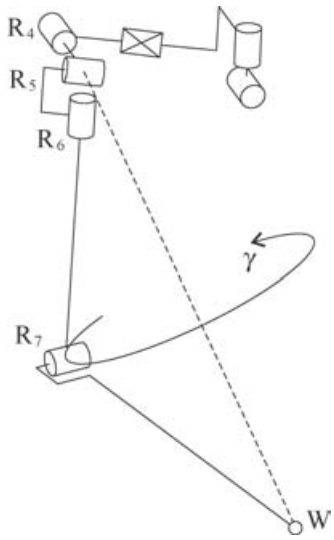

Fig. 8. Self-motion of humanoid mechanism with fixed inner shoulder joint.

coplanar[11] and one can identify a humanoid ratio between the produced inclination angles. Still, there exist self-motions of the shoulder complex that do not disturb the upper arm orientation, such as the shrugging motion. These, however, are not typical when the primary task of the arm is to position the wrist.

For the sake of simplicity let us lock the inner shoulder joint and observe the motion of the outer shoulder joint in combination with the elbow. A spatial position of point W can be achieved with an infinite number of orientations of the upper arm[20] as shown in Fig. 8. For a fixed position of the wrist point W, the self-motion of a humanoid arm consists of the rotation of the elbow center point through an angle γ about an axis that passes through the center of the outer shoulder joint and point W. In this motion the elbow angle q_7 remains constant. This self-motion ability is very important for a humanoid arm because introduces a freedom of choosing best configurations with respect to given secondary tasks. Non-redundant mechanisms do not possess this ability and are, therefore, less adaptable and versatile.

The degree of redundancy of the simplified kinematic arrangement in Fig. 8 is one and the quantity of the self-motion of the mechanism can, therefore, be expressed in terms of one parameter, for instance, by measuring the range of angle γ. In humans, this range varies throughout the workspace (between 90° and 120°) and is typically higher in the central region of the workspace. A more correct mathematical way to quantify one degree of redundancy is to evaluate the so-called self-motion curves.[21] In our case, they can easily be plotted in three-dimensional space of coordinates q_4, q_5, q_6 because q_7 is a constant parameter[20] for a given position of W.

The problem with redundancy is that the self-motion domain can in general be composed of a number of subspaces – disconnected curves. Each of these corresponds to one group of inverse kinematics solutions where one group of solutions may contain an optimum configuration to solve the secondary task, while other groups may not. Without violating the prescribed primary task constraints (without changing the position of point W), the arm cannot switch from one group of solutions to another and the secondary task may not be solved in the best possible way.

A deeper numerical analysis shows that the mechanism in Fig. 8 possesses eight disconnected self-motion curves. However, for the imposed humanoid joint limits the arm can utilize only one self-motion curve, which is only one eight of the entire theoretical self-motion capacity of this mechanism. The good news is that this simplifies the strategy how to resolve and utilize the kinematic redundancy when solving different secondary tasks, such as the minimization of joint torques or others.

III.4. Optimum arm configurations

Even though the quantity of the self-motion of a humanoid arm seems relatively small it cannot be disregarded. We can demonstrate that the performances of a humanoid arm significantly depend on its self-motion ability. An illustrative example is the distribution of the manipulability ellipsoids in the arm's workspace. It is well known that the manipulability ellipsoids connect the joint velocities with the end effector velocities (with the translational velocities of point W). The longest principal axis of the manipulability ellipsoid shows the direction and the amplitude of the maximum velocity of the wrist. Manipulability ellipsoids also connect the outside force applied to the wrist with the corresponding joint torques. The joint torques are minimized when the force is applied in the direction of the shortest principal axis of the manipulability ellipsoid. In a singular configuration, the manipulability ellipsoid collapses in at least one direction. If the force is applied in that direction, the joint torques will be zero and the manipulator will resist to an infinite outside force.

An advantage of a redundant humanoid arm is that it is possible to change the geometry of the manipulability ellipsoids by the self-motion with the wrist point W fixed in a desired spatial position. The shapes and sizes of the manipulability ellipsoids were studied in reference [22]. We showed that the arm is capable to simultaneously produce very flat and very round manipulability ellipsoids in the workspace region that is close to the shoulder as presented in Fig. 9. The manipulability ellipsoids are flat if the elbow is positioned downward. This is statically the best configuration for resisting vertical outside forces (weights). When the elbow is upward, the manipulability ellipsoids become very round. In this configuration, the mechanism can provide uniform velocities of the wrist in all directions. Such a

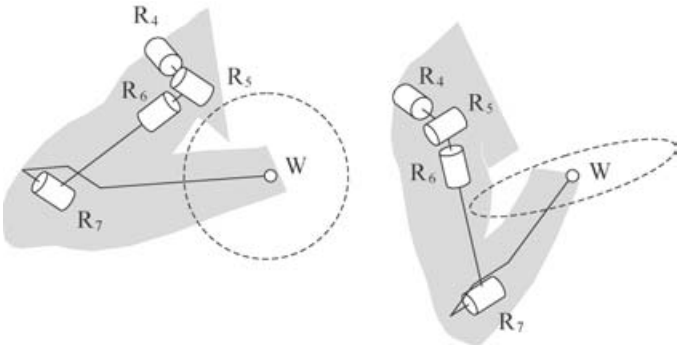

Fig. 9. Optimum arm configurations to obtain most round and most flat manipulability ellipsoid in same position of point W.

https://doi.org/10.1017/S0263574705001906 Published online by Cambridge University Press

property can be utilized to execute a variety of tasks that request fine and precise movements of the wrist. A number of similar examples could be found with the human arm solving different tasks.

By changing the configuration along the self-motion curve a humanoid arm can increase its rigidity or compliance and can gain mechanical advantage near kinematic singularities. Weak actuation can be compensated by a more sophisticated control that exploits singularities. In contrast to this humanoid control strategy, conventional control schemes for robots are aimed to avoid singularities because they provoke undesired ill-conditioned motion and infinite joint velocities. A deeper analysis of humanoid motion can also bring into light new principles in the design of robot manipulators. It can be shown, for instance,[23] that by using a control that exploits singularities in the weight lifting task, the joint torques in the elbow are much higher than those in the shoulder. This seems paradoxical for conventional robot design, in humans, however, the elbow joint appears to be stronger than the shoulder joint.

IV. CONCLUSIONS

Positional abilities of a humanoid arm are studied in this paper. A kinematical model which was synthesized from a number of electro-optical measurements of healthy female and male subjects is utilized for this purpose. The main vantage of the model is in the usage of two displaced spherical joints in the shoulder complex and in the usage of joint limits as functions of joint coordinates. This enables us to compute and replicate human manipulation characteristics more accurately.

In this paper, we determine the reachability of a humanoid arm, we treat the orienting redundancy in the shoulder complex and the positional redundancy in the shoulder-elbow complexes, and present optimum configurations in executing a task which requires uniform velocities in all directions and a task which requires supporting heavy loads.

We believe that the kinematic arrangement of a humanoid arm, ranges of motion in joints, kinematic redundancy and distribution of singularities are very important to be studied and understood. These properties significantly contribute to the motion abilities of a humanoid arm and must be considered in the design and control of humanoid robots. Moreover, we can foresee applications in medicine and sports, in particular in physiotherapy and ergonomics.

Acknowledgements

The authors are grateful to the Ministry of Education, Science and Sports, Republic of Slovenia, for the support of this investigation.

References

1. K. Hirai, "Current and future perspective of Honda humanoid robot," *Proc. IEEE Int. Conf. Intell. Robot and Syst.* (1997) pp. 500–508.
2. J. Yamaguchi, S. Inoue, D. Nishino and A. Takanishi, "Development of a bipedal humanoid robot having antagonistic driven joints and three dof trunk," *Proc. IEEE Int. Conf. Intell. Robot and Syst.* (1998) pp. 96–101.
3. D. Tolani, A. Goswami and N. I. Badler, "Real-time inverse kinematics techniques for anthropomorphic limbs," *Graphical Models* **62**, 353–388 (2000).
4. T. B. Moeslund and E. Granum, "Modelling and estimating the pose of a human arm," *Machine Vision and Applications* **14**, 237–247 (2003).
5. E. Pennestri, A. Renzi and P. Santonocito, "Dynamic modeling of the human arm with video-based experimental analysis," *Multybody System Dynamics* **7**, 389–406 (2002).
6. M. A. Admiraal, M. J. M. A. M. Kusters and S. C. A. M. Gielen, "Modelling kinematics and dynamics of human arm movements," *Motor Control* **8**, 312–338 (2004).
7. E. V. Biryukova, A. Roby-Brami, A. A. Frolov and M. Mokhtari, "Assesment of the accuracy of a human arm model with seven degress of freedom," *J. of Biomechanics* **33**, 985–995 (2000).
8. R. A. Prokopenko, E. V. Biryukova, A. A. Frolov, E. V. Biryukova and A. Roby-Brami, "Kinematics of human arm reconstructed from spatial tracking system recordings," *J. of Biomechanics* **34**, 177–185 (2001).
9. M. Okada, Y. Nakamura and S. Hoshino, "Development of the cybernetic shoulder – A three DOF mechanism that imitates biological shoulder-motion," *Proc. of IEEE Int. Conf. on Intell. Robot Syst.* (1999) pp. 543–548.
10. A. E. Engin and S. T. Tumer, "Three-dimensional kinematic modeling of the human shoulder complex – part I: Physical model and determination of joint sinus cones," *Trans. of the ASME J. of Biomech. Eng.* **111**, 107–112 (1989).
11. J. Lenarčič and M. M. Stanišić, "A humanoid shoulder complex and the humeral pointing kinematics," *IEEE Trans. on Robotics and Automat.* **19**, No. 3, 499–506 (2003).
12. J. Lenarčič, M. M. Stanišić and V. Parenti-Castelli, "Kinematic design of a humanoid robotic shoulder complex," *Proc. Int. Conf. on Robotics and Automat.*, San Francisco, CA (2000) pp. 27–32.
13. N. Klopčar and J. Lenarčič, "Accurate kinematical model for the determination of human arm reachable workspace," *Meccanica* (in print).
14. A. E. Engin, "On the biomechanics of the shoulder complex," *J. of Biomechanics* **13**, 575–590 (1980).
15. Z. Dvir and N. Berme, "The shoulder complex in elevation on the arm: a mechanism approach," *J. of Biomech.* **11**, 219–225 (1987).
16. J. Hesselbach, M. B. Helm, H. Kerle, M. Frindt and A. M. Weinberg, "Kinematics of the human forearms pro- and supination," *Advances in Robot Kinematics: Analysis and Control* (Kluwer Academic Publishers, J. Lenarčič and M. L. Husty, Eds., 1998), pp. 551–560.
17. J. Lenarčič and A. Umek, "Simple model of human arm reachable workspace," *IEEE Trans. System, Man and Cybernetics* **22**, 1239–1246 (1994).
18. D. A. Winter, *Biomechanics and Motor Control of Human Movement* (Wiley-Interscience Publication, University of Waterloo, 1990).
19. J. Lenarčič, U. Stanič and P. Oblak, "Some kinematic considerations for the design of robot manipulators," *Robotics and Computer-Integrated Manufacturing* **5**, Nos. 2/3, 235–241 (1989).
20. J. Lenarčič, "The self-motion of an anthropomorphic manipulator," *Advances in Robot Kinematics: Analysis and Control* (Kluwer Academic Publishers, J. Lenarčič and M. L. Husty, Eds., 1998) pp. 571–578.
21. J. W. Burdick, "On the inverse kinematics of redundant manipulators: Characterization of the self-motion manifolds," *Proc. of Int. Conf. on Robotics and Automation ICRA-89*, Scottsdale, AZ (1989) pp. 264–270.
22. J. Kieffer and J. Lenarčič, "On the exploitation of mechanical advantage near robot singularities," *Informatica* **18**, 315–323 (1994).
23. J. Lenarčič, "Basic kinematic characteristics of humanoid manipulators," *Laboratory Robotics and Automation* **11**, No. 5, 272–278 (1999).